EurJIC European Journal of Inorganic Chemistry

ChemPubSoc Europe

FULL PAPER

DOI:10.1002/ejic.201300176

Implementing Liquid-Crystalline Properties in Single-Stranded Dinuclear Lanthanide Helicates

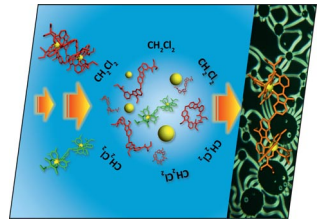

COVER PICTURE

Emmanuel Terazzi,*[a] Amir Zaïm,[a] Bernard Bocquet,[a] Johan Varin,[a] Laure Guénée,[b] Thibault Dutronc,[a] Jean-François Lemonnier,[a] Sébastien Floquet,[c] Emmanuel Cadot,[c] Benoît Heinrich,[d] Bertrand Donnio,[d] and Claude Piguet*[a]

Keywords: Liquid crystals / Metallomesogens / Polynuclear complexes / Amphiphiles / Helical structures / Lanthanides

The connection of flexible protodendritic wedges to the bis-tridentate rigid polyaromatic ligand **L1** provides amphiphilic receptors **L5** and **L6**; their reduced affinities for complexing trivalent lanthanides (Ln = La, Y, Lu) in organic solvent (by fifteen orders of magnitude!) prevent the formation of the expected dinuclear triple-stranded helicates $[Ln_2(\mathbf{L}\boldsymbol{k})_3]^{6+}$. This limitation could be turned into an advantage because **L1** or **L6** can be treated with $[Ln(hfac)_3]$ (Hhfac = 1,1,1,5,5,5-hexafluoro-2,4-pentanedione) to give neutral single-stranded $[Ln_2(\mathbf{L}\boldsymbol{k})(hfac)_6]$ complexes with no trace of higher-order helicates. Whereas ligands **L1** and **L5** are not liquid crystals, **L6** can be melted above room temperature (41 °C) to give a nematic mesophase, and its associated dinuclear helical complex $[Y_2(\mathbf{L6})(hfac)_6]$ self-organises at the same temperature into a fluidic smectic mesophase.

Introduction

For a long time, lanthanide supramolecular chemistry focused on the design and on the thermodynamic rationalisation of discrete sophisticated polynuclear molecular architectures such as helicates,[1] cages,[2] clusters[3] and grids.[4] Owing to the remarkable magnetic and optical properties associated with the 4f-centred open-shell electronic configurations, these compounds were approached for overcoming modern technological limitations, but the exploitation of their intrinsic properties for lighting, sensing and switching further requires specific patterns gained by the self-organisation of amphiphilic receptors connected to the inorganic cores.[5,6] When the organic coating induces liquid-crystalline properties, the resulting metal-containing liquid crystals are referred to as metallomesogens,[7] or more specifically, as lanthanidomesogens for those that incorporate metallic cations with $[Xe]4f^n$ configurations.[8] Roughly speaking, most thermotropic liquid crystals (i.e., liquid crystals that self-organise with temperature) are produced by connecting long and flexible aliphatic chains to various rigid polarisable aromatic cores.[9] Optimisation of the intermolecular interactions in the crystalline state results in a microsegregation process, in which the rigid cores are packed together, whereas the less polarisable flexible alkyl chains fill the residual voids of the structure.[10] Upon heating, the decorrelation between the flexible alkyl chains produces a molten continuum (assigned to the melting process), with the residual interactions between aromatics ensuring the stability of the liquid-crystalline phase. At higher temperature, the interactions between the aromatic units become smaller than the thermal energy and a classical liquid is obtained (assigned to the isotropisation process). This standard two-step melting model satisfyingly predicts the thermal behaviour of low-molecular-weight amphiphilic organic molecules that possess considerable anisometric shapes.[10,11] In metallomesogens, the isotropic three-dimensional expansion brought by the coordination spheres of the metals usually disrupts the microsegregation and destabilises the liquid-crystalline phase. Except for complexes with linear or square-planar arrangements that are reminiscent of the molecular shapes found in purely organic liquid crystals,[7,12] common coordination geometries are difficult to combine with the structural anisotropy required for inducing mesomorphism and liquid-crystalline phases are not formed. In this context, only a few metallomesogens contain a tetrahedral[13] or an octahedral metal centre,[14] and

[a] Department of Inorganic and Analytical Chemistry, University of Geneva,
30 quai E. Ansermet, 1211 Geneva 4, Switzerland
E-mail: Emmanuel.Terazzi@unige.ch
Claude.Piguet@unige.ch
Homepage: http://www.unige.ch/sciences/chiam/piguet/Welcome.html
[b] Laboratory of Crystallography, University of Geneva,
24 quai E. Ansermet, 1211 Geneva 4, Switzerland
[c] Institut Lavoisier de Versailles, UMR 8180,
University of Versailles Saint-Quentin,
45 av. des Etats-Unis, 78035 Versailles, France
[d] Institut de Physique et Chimie des Matériaux de Strasbourg (IPCMS), UMR 7504 (CNRS – Université de Strasbourg),
23 rue du Loes, BP43, 67034 Strasbourg cedex 2, France

Supporting information for this article is available on the WWW under http://dx.doi.org/10.1002/ejic.201300176.

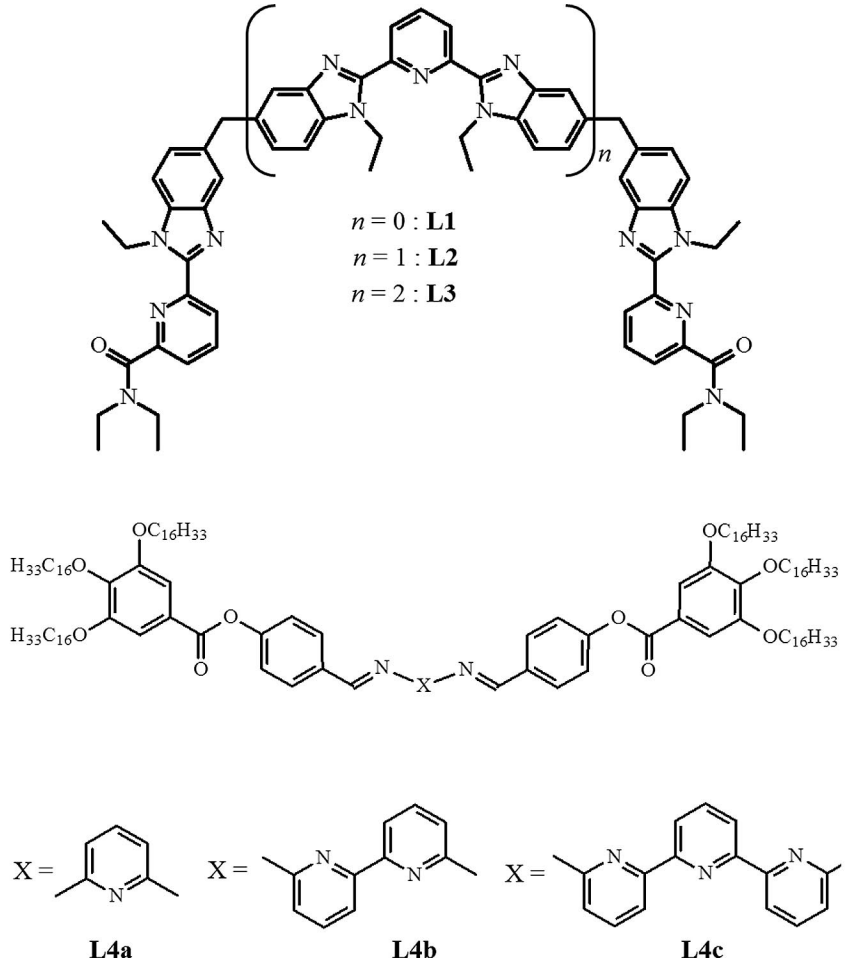

L4a **L4b** **L4c**

those with coordination number (CN) 7–12, typical of large lanthanide cations, have remained challenging for some time.[5,15] Pioneering work dedicated to fullerodendrimers[16] established that mesomorphism could be induced when the bulky spherical cores were coated with divergent polarised dendritic architectures, a strategy that led to the preparation of a unique discotic dinuclear lanthanidomesogen.[15d] To the best of our knowledge, there is no other report of multinuclear mesomorphic analogues despite a rich catalogue of polynuclear linear triple-stranded helicates such as $[Ln_2(\mathbf{L1})_3]^{6+}$, $[Ln_3(\mathbf{L2})_3]^{9+}$ and $[Ln_4(\mathbf{L3})_3]^{12+}$, the cylindrical rigid cores of which make them ideal for the design of calamitic metallomesogens.[1]

However, by following this strategy, lipophilic dinuclear helicates with d-block metals $[Cu_2(\mathbf{L4}n)_2]^{2+}$ (n = a, b, c) have been shown to self-organise into columnar mesophases.[13b,17] Interestingly, the connection of the long lipophilic and diverging alkyl chains to the cylindrical core drastically limited the stability of these complexes in solution, an observation that might explain the paucity of helical scaffolds in metallomesogens. To extend this approach to magnetically and optically active 4f-block cations, we connect here two different lipophilic protomesomorphic dendrons perpendicularly to the helical axis in **11** through ether links (**L5**) or ester bonds (**L6**) (Scheme 1). The conditions required for the preparation of stable dinuclear lanthanidomesogens are explored together with their liquid-crystalline properties.

Results and Discussion

Synthesis of Ligands Lk (k = 5, 6) and Formation of the Triple-Stranded Complexes $[Ln_2(L\mathit{k})_3(CF_3SO_3)_6]$ (Ln = La, Y, Lu; k = 5, 6) in Solution

Alkylation of intermediate **11** with **15** gave the target ligand **L5**, whereas esterification with **16**[15i] yielded **L6** (Scheme 1 and Appendix 1 in the Supporting Information).

The five different ^{1}H NMR spectroscopic signals detected for the aromatic protons Hb–Hf in Lk (k = 5, 6), combined with the observation of a singlet for the protons Ha and of a quartet for the protons Hm, confirmed the existence of dynamically averaged C_{2v} symmetries for the free ligands in solution (see Scheme 1 for numbering). The lack of a nuclear Overhauser enhancement (NOE) effect between the ethyl residues of the benzimidazole rings and the protons connected at the 3-positions of the pyridine rings agreed with a standard *trans* arrangement of the N-donor atoms borne by the adjacent aromatic rings. This arrangement was confirmed by analysis of the solid-state structure

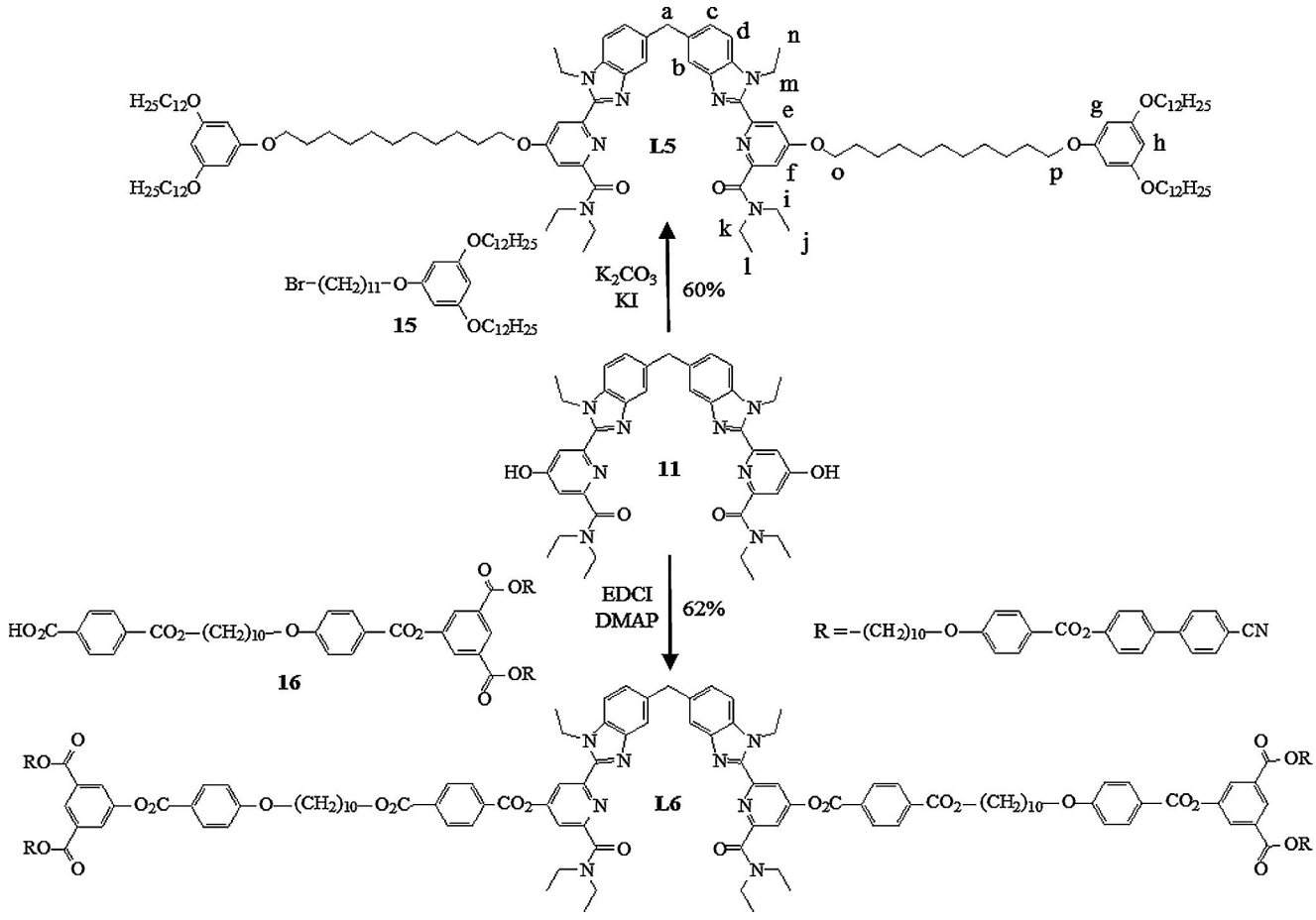

Scheme 1. Synthesis and structures of bis-tridentate ligands **L5** and **L6**, derived from **11** (with numbering scheme for NMR spectra).

of intermediate **10** (Appendix 1 in the Supporting Information). Reaction of the bis-tridentate ligand **L6** (3 equiv.) with $[Y(CF_3SO_3)_3]\cdot 4H_2O$ (1 equiv.) in CD_2Cl_2 provided a temperature-independent broad ^1H NMR spectrum (Figure S2a in the Supporting Information) that indicates weak interactions between the binding unit and the central diamagnetic Y^{3+} cation, which leads to the formation of intricate mixtures of complexes in intermediate exchange on the NMR spectroscopic timescale. The use of more polar solvents ($CDCl_3$, CD_3NO_2, $[D_8]$THF; Figure S2b) did not improve the situation and the ESI-MS spectrum of the colourless mixture only showed the presence of the protonated free ligand $[\mathbf{L6} + H]^+$. Since the bis-tridentate ligand **L1** is known to produce very stable triple-helical complexes $[Ln_2(\mathbf{L1})_3](CF_3SO_3)_6$ in acetonitrile [log ($\beta_{2,3}^{\mathbf{L1}}$ ≅ 25)],[18] this deleterious effect can be tentatively assigned to the considerable lipophilicity of **L6**, which is efficiently solvated in organic solvents. Upon reaction of the less lipophilic ligand **L5** (3 equiv.) with $[Y(CF_3SO_3)_3]\cdot 4H_2O$ (1 equiv.) in CD_2Cl_2/CD_3CN = 1:4, the six metal-shifted ^1H NMR spectroscopic signals observed for the aromatic protons Hb–Hh were diagnostic for overall threefold symmetry.[19] The helical arrangement of the strands was substantiated by the detection of pseudo-sextets [ABX_3 spin systems for which $^2J = 2\cdot(^3J)$] for the diastereomeric methylene protons of the ethyl residues (Hm), whereas the singlet (A_2 spin system) observed for the enantiotopic methylene protons (Ha) of the diphenylmethane spacer points to the existence of three twofold axes perpendicular to the threefold axis in line with the regular D_3-symmetrical triple-helical arrangement of the expected triple-stranded helicate $[Y_2(\mathbf{L5})_3]^{6+}$ (Figure 1, a). Upon addition of increasing amounts of CD_2Cl_2, the signals of the complex were broadened because of partial ligand dissociation and slow exchange processes (Figure 1b–h and Figure S3 in the Supporting Information), a trend that was confirmed by the decreasing ratio of the peaks detected by ESI-MS spectra for $[Y_2(\mathbf{L5})_3(CF_3SO_3)_n]^{(6-n)+}$ and $[\mathbf{L5} + H]^+$, respectively. We conclude that the reduced lipophilicity in **L5** limits the solvation of the free ligand to such an extent that $[Y_2(\mathbf{L5})_3]^{6+}$ can be obtained in polar organic solvents at millimolar concentrations [see Equilibrium (1) below].

If we take the integral I_{gh} of the ^1H NMR spectral singlet recorded for the peripheral aromatic protons Hg,Hh as a probe for calibrating the total ligand concentration in each mixture ($|\mathbf{L5}|_{tot} = |\mathbf{L5}| + 3|[Y_2(\mathbf{L5})_3]|$), the stability constants $\beta_{2,3}^{Ln,\mathbf{L5}}$ for Equilibrium (1) can be estimated by integration

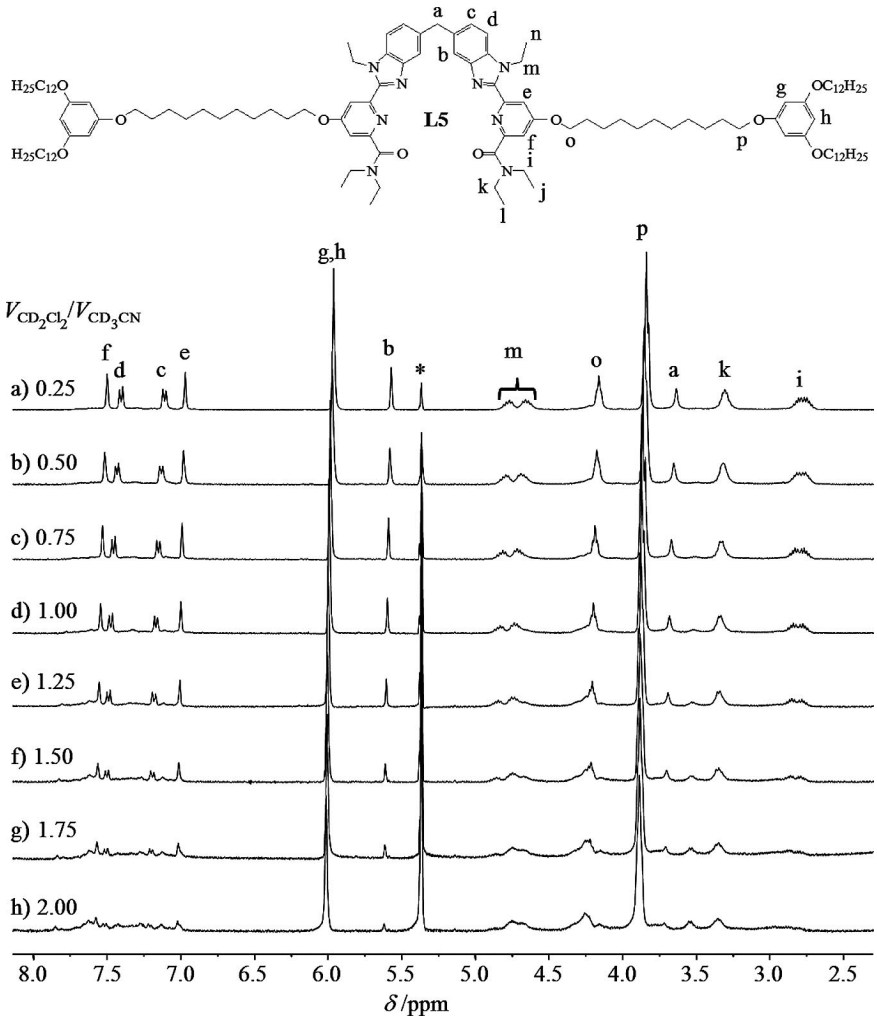

Figure 1. ^{1}H NMR spectra with numbering scheme of the diamagnetic triple-stranded helicate $[Y_2(\mathbf{L5})_3]^{6+}$ at different $V_{CD_2Cl_2}/V_{CD_3CN}$ volume; * = $CDHCl_2$ (total ligand concentration $|\mathbf{L5}|_{Tot}$ ≅ 0.01 M, 298 K).

of the signals recorded for proton b (I_b) in each solvent mixture (Table 1).

$$3\mathbf{L5} + 2Ln(CF_3SO_3)_3 \rightleftharpoons [Ln_2(\mathbf{L5})_3](CF_3SO_3)_6 \ \beta_{2,3}^{Ln,\mathbf{L5}} \quad (1)$$

The stability constants estimated for $[Ln_2(\mathbf{L5})_3](CF_3SO_3)_6$ are more than fifteen orders of magnitude smaller than those found for the parent nonlipophilic complexes $[Ln_2(\mathbf{L1})_3](CF_3SO_3)_6$ in pure acetonitrile (Figures S4–S9 in the Supporting Information).[18] These thermodynamic data unambiguously demonstrate that the efficient solvation of ligand **L*k*** (k = 5, 6) in organic solvents severely limits their affinity for trivalent lanthanides, but the presence of a significant amount of CH_2Cl_2 is crucial for the solubilisation of these ligand. These two conflicting requirements prevent the isolation of pure triple-stranded lipophilic helical lanthanide complexes, which results from the successive

Table 1. Experimental cumulative formation constants $\log(\beta_{2,3}^{Ln,\mathbf{L5}})$ obtained by ^{1}H NMR spectroscopy according to Equilibrium (1) (Ln = La, Y and Lu; total concentration of ligand $|\mathbf{L5}|_{tot}$ = 0.01 M).[a]

$V_{CD_2Cl_2}/V_{CD_3CN}$	$\log(\beta_{2,3}^{La,\mathbf{L5}})$ $[La_2(\mathbf{L5})_3](CF_3SO_3)_6$	$\log(\beta_{2,3}^{Y,\mathbf{L5}})$ $[Y_2(\mathbf{L5})_3](CF_3SO_3)_6$	$\log(\beta_{2,3}^{Lu,\mathbf{L5}})$ $[Lu_2(\mathbf{L5})_3](CF_3SO_3)_6$
0.25	8.8(1)	10.1(1)	9.5(2)
0.50	8.3(1)	9.8(2)	8.4(1)
0.75	7.4(1)	9.6(2)	7.7(1)
1.00	7.1(2)	9.1(1)	7.1(2)
1.25	6.4(4)	8.9(1)	6.5(4)
1.50	5(1)	8.3(1)	4.4(4)
1.75	_[b]	7.3(2)	5.9(8)
2.00	_[b]	7.1(3)	_[b]

[a] The standard deviations are calculated for integration uncertainties of 5%. [b] The signals of the complexes are too weak to be detected.

fixation of three tridentate binding unit about each metal. However, this drawback can be turned into an advantage with the lipophilic ligand **L6**, which possesses the structural criteria for designing lanthanidomesogens. Indeed, the replacement of poorly coordinating triflate anions with hexafluoroacetylacetonate (hfac) anions should strictly limit the affinity of the central metal to a single tridentate binding unit, as found in [Ln(**L*k***)(hfac)$_3$] (*k* = 7, 8),[20] thus leading to the formation of the single-stranded [Ln$_2$(**L6**)(hfac)$_6$] complexes with no possible mixing with higher-order helicates.

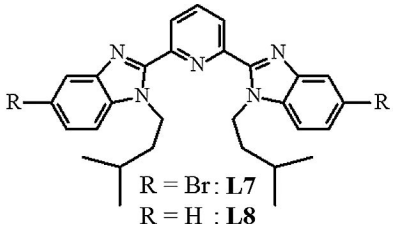

Synthesis and Structure of the Single-Stranded Complexes [Ln$_2$(L*k*)(hfac)$_6$] (*k* = 1, 6; Ln = Y, Lu)

Reaction of the C_{2v}-symmetrical bis-tridentate ligand **L1** (1 equiv.) with [Lu(hfac)$_3$(diglyme)] (2 equiv.) in acetonitrile followed by the slow diffusion of diethyl ether yielded small colourless crystals suitable for X-ray analysis (Tables S4–S6 in the Supporting Information). No standard hydrogen bonds or intermolecular stacking interactions could be found, and the molecular structure confirmed the coordination of one Lu^{III} ion to each *cis–cis* tridentate segment of ligand **L1**, thus leading to an intramolecular intermetallic Lu···Lu separation of 12.533(1) Å (Figure 2). Each Lu^{III} cation is almost held within the equatorial plane defined by the three donor atoms of each tridentate binding unit (O1, N1, N3 for Lu1 and O2, N5, N7 for Lu2; deviations of the Lu atom from the planes: 0.009 and 0.018 Å, respectively). Each coordination sphere is completed with three didentate hfac anions, with two of them being located on both sides of the equatorial plane and the third roughly perpendicular (81.4–84.1°) to the latter plane. This results in pseudo-C_{2v} symmetry around the lutetium ion, an arrangement that is compatible with the description of the nine-coordinate coordination spheres as distorted mono-capped square antiprisms with N1 (Lu1) or N5 (Lu2) occupying the capping positions (Figure S10 and Tables S7–S8 in the Supporting Information). The average distances Lu1–O = 2.34(5) Å, Lu1–N = 2.477(4) Å, Lu2–O = 2.35(5) Å and Lu2–N = 2.502(8) Å (Table S5 in the Supporting Information) are close to those found in the mononuclear analogues [Lu(**L*k***)(hfac)$_3$] (*k* = 7, 8),[20] an observation that is corroborated by the calculated bond valences (Table S9 in the Supporting Information).[21] The helicity of the diphenylmethane spacer, defined as a five-atom crooked line (C15–C14–C20–C21–C27) amounts to *H* = 0.55,[22] a value that is in line with *H* = 0.76 reported for the analogous single-stranded complex [Eu$_2$(**L1**)(NO$_3$)$_6$(H$_2$O)$_2$].[23]

Monitoring the titration of **L6** with [Y(hfac)$_3$(diglyme)] in CDCl$_3$ by using ^{1}H NMR spectroscopy showed the stepwise formation of the complexes [Y(**L6**)(hfac)$_3$] and [Y$_2$(**L6**)(hfac)$_6$] according to Equilibria (2) and (3) (Figures S11–S17 in the Supporting Information). The broadened ^{1}H NMR spectroscopic signals implied the operation of intermolecular exchange processes with an intermediate rate on the NMR spectroscopic timescale but the concomitant observation of a singlet for the protons of the three complexed hfac anions indicated fast intramolecular exchange between axial and meridional positions in [Y(**L6**)(hfac)$_6$] and [Y$_2$(**L6**)(hfac)$_6$].

$$\mathbf{L6} + [Y(hfac)_3(diglyme)] \rightleftharpoons [Y(\mathbf{L6})(hfac)_3] + diglyme \quad \beta_{1,1}^{Y(hfac)_3,\mathbf{L6}} \tag{2}$$

$$\mathbf{L6} + 2[Y(hfac)_3(diglyme)] \rightleftharpoons [Y_2(\mathbf{L6})(hfac)_6] + 2\,diglyme \quad \beta_{2,1}^{Y(hfac)_3,\mathbf{L6}} \tag{3}$$

A thorough analysis of the ^{1}H NMR spectroscopic signals for the Y^{III}/**L6** = 2.0 ratio in chloroform revealed the

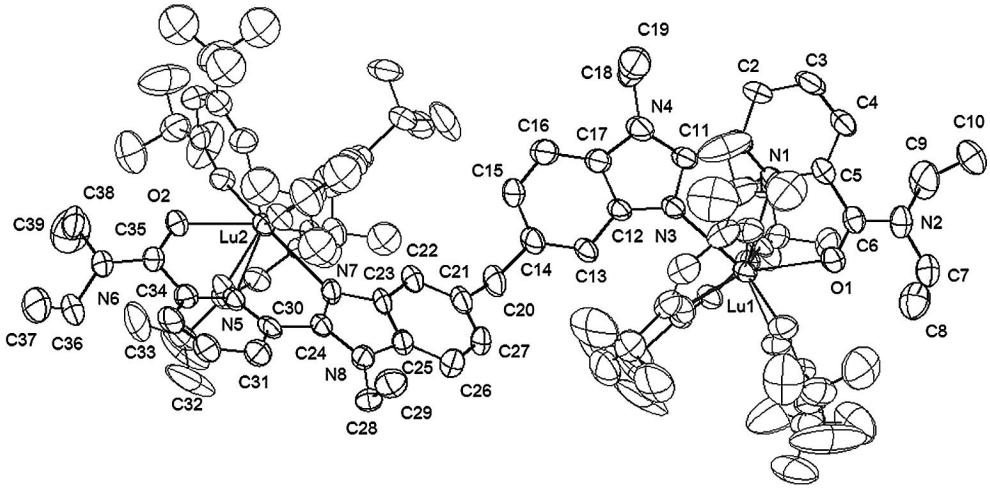

Figure 2. Perspective view with numbering scheme of the molecular structure of [Lu$_2$(**L1**)(hfac)$_6$]. Ellipsoids are represented at 50% probability level. The labels for hfac and the hydrogen atoms are omitted for clarity.

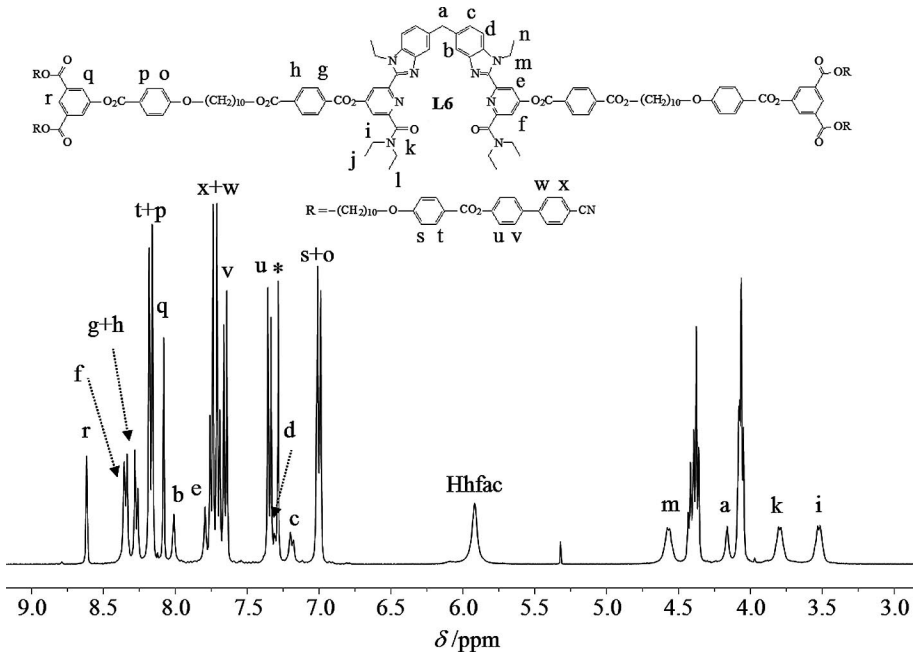

Figure 3. ^{1}H NMR spectrum with numbering scheme of the diamagnetic complex [Y_2(**L6**)(hfac)$_6$] ($CDCl_3$, 298 K); * = $CHCl_3$.

existence of a single complex in solution with a pattern of five signals for the aromatic protons Hb–Hf (twofold symmetry) and the presence of a singlet for the enantiotopic methylene protons Ha (planar symmetry) that are diagnostic of an average C_{2v}-symmetrical arrangement of the coordinated ligand strand in [Y_2(**L6**)(hfac)$_6$] (Figure 3).

Nonlinear least-squares fit[24] of the dynamically averaged ^{1}H NMR spectroscopic titration data provided complete sets of chemical shifts for [Y(**L6**)(hfac)$_6$] and [Y_2(**L6**)(hfac)$_6$] (Table S10 in the Supporting Information) together with cumulative stability constants $\log[\beta_{1,1}^{Y(hfac)_3,\mathbf{L6}}]$ = 6(2) and $\log[\beta_{2,1}^{Y(hfac)_3,\mathbf{L6}}]$ = 11(2), which agreed with $\log[\beta_{1,1}^{Ln(hfac)_3,\mathbf{Lk}}] \geq 5.7$ estimated for the mononuclear complexes [Ln(**L*k***)(hfac)$_3$] (*k* = 7, 8; Ln = La, Eu, Lu, Y) in $CDCl_3$.[20] The pure single-stranded dinuclear [Y_2(**L6**)-(hfac)$_6$]·29H_2O complex could be eventually obtained by treating **L6** (1 equiv.) with [Y(hfac)$_3$(diglyme)] (2 equiv.) in $CHCl_3$ followed by precipitation with hexane (Table S1 in the Supporting Information).

Liquid-Crystalline Organisation of Ligand L6 and Its Complex [Y_2(L6)(hfac)$_6$]

The thermal behaviours of ligand **L6** and its yttrium complex [Y_2(**L6**)(hfac)$_6$] were studied by a combination of polarised optical microscopy (POM), thermogravimetric analysis (TGA) and differential scanning calorimetry (DSC) measurements (Figure 4, Table 2 and Figures S18–20 in the Supporting Information). Temperature-dependent POM observations (20–250 °C temperature range) showed the formation of fluid birefringent textures for **L6** and [Y_2(**L6**)(hfac)$_6$] upon heating (Figure S18) that are typical of the occurrence of liquid-crystalline organisations, whereas ligand **L5** did not show any birefringence in solid

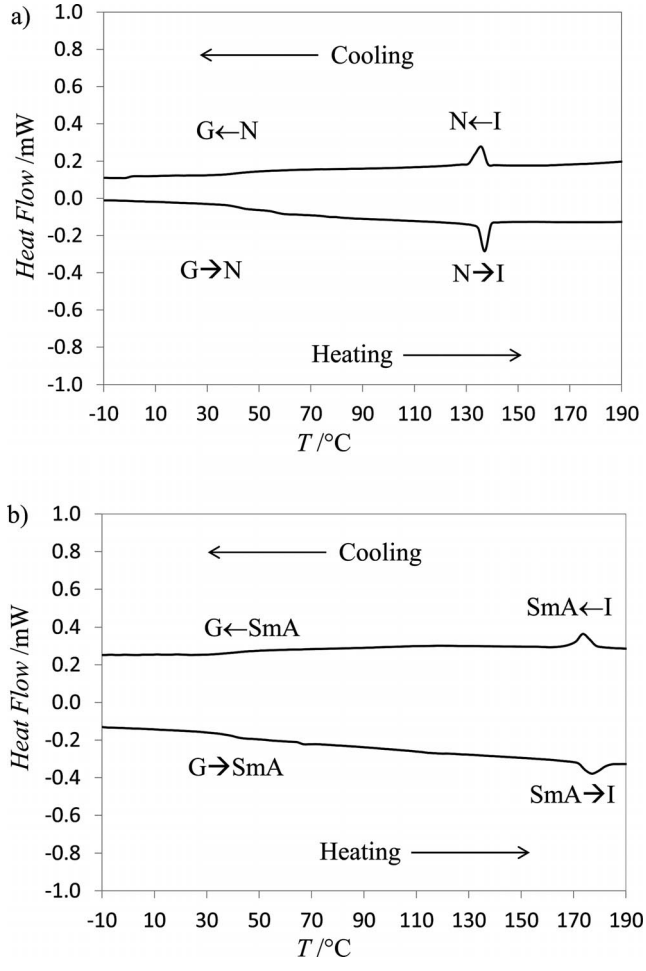

Figure 4. (a) DSC trace of the ligand **L6** at 5 °C min^{-1}; (b) DSC trace of complex [Y_2(**L6**)(hfac)$_6$] at 5 °C min^{-1} (second heating and cooling).

or in liquid states. The optical defects observed in the liquid-crystalline texture of ligand **L6** were typical of a nematic phase (N) (Figure S18a), whereas the observation of homeotropic zones for $[Y_2(\mathbf{L6})(hfac)_6]$ suggested the formation of a more ordered smectic A (SmA) phase (Figure S18b).

Table 2. Temperatures, enthalpy and entropy changes of the phase transitions observed for ligands **L*k*** (*k* = 5, 6) and complex $[Y_2(\mathbf{L6})(hfac)_6]$.

Compound	Phase sequence[a]	Transition temp. *T* [°C]	ΔH [kJ mol^{-1}]	ΔS [J mol^{-1} K^{-1}]
L5	G → I	–30	–	–
L6[b]	G → N	41	–	–
	N → I	134	16.2	39.8
$[Y_2(\mathbf{L6})(hfac)_6]$[b]	G → SmA	40	–	–
	SmA → I	172	15.8	35.5

[a] G = glassy state, N = nematic phase, SmA = smectic A phase, I = isotropic fluid. [b] The liquid-crystalline phases were identified from their optical textures by POM and from small angle (SA) XRD studies. Temperatures are given for the onset of the peaks observed during the second heating processes.

DSC measurements confirmed these observations. Ligand **L5** transformed directly through a low-temperature glass transition into an isotropic liquid, which was then stable up to 350 °C (Table 2 and Figure S19 in the Supporting Information). For ligand **L6** and its dinuclear complex $[Y_2(\mathbf{L6})(hfac)_6]$, glass transitions (centred around 40 °C for both compounds) led to the mesophases, which were then transformed into isotropic liquid through first-order transitions at higher temperature (Figure 4, Table 2). After the first heating, during which co-crystallised molecules of water were lost (Figure S20 in the Supporting Information), these two mesomorphic compounds showed a good thermal stability (i.e., no weight loss is observed by TGA and the complex remained unchanged by POM) together with a reversible thermal behaviour over several heating/cooling cycles (5 °C min^{-1} under N_2).

Temperature-dependent SAXRD patterns were recorded for **L6** and $[Y_2(\mathbf{L6})(hfac)_6]$ in the 20–200 °C range (Figures S21–25 in the Supporting Information). In both cases, the presence of a large and diffuse signal at approximately 4.5 Å, which was associated with the liquidlike lateral ordering of the molten chains and mesogenic cores, confirmed the fluidlike nature of the mesophases. No sharp small-angle reflection could be detected for **L6**, only a broad scattering, that, along POM observation, corroborated the induction of the nematic liquid-crystalline phase. The diffractogram collected at 120 °C for $[Y_2(\mathbf{L6})(hfac)_6]$, taken as a representative example, showed two sharp small-angle reflections in the ratio 1:2, which was characteristic of 1D lamellar ordering (the reflections were indexed with the 001 and 002 Miller indices), and the position of which gave a weakly temperature-dependent periodicity of d = 105 Å. This periodicity in $[Y_2(\mathbf{L6})(hfac)_6]$ is shorter (i) than the total length of **L6** in its extended conformation (estimated to be about 130 Å; see Figure S26 in the Supporting Information) and (ii) than the periodicity previously reported for the SmA phases ($d \approx 120$ Å) produced by the related mononuclear dendritic complexes $[Ln_2(\mathbf{L9})(NO_3)_6]$ and $[Ln_2(\mathbf{L10})(NO_3)_6]$ (see Figure S26).[15i–15j]

The abnormal intensity profile displayed by the two reflections (Figures S22–S24 in the Supporting Information) with a relatively weak (001) reflection with respect to (002) involves the alternation of several high-electronic density sublayers, hence the central metallic fragment and the branching and peripheral mesogens, with low-electronic density sublayers associated with the C10 aliphatic spacers (Figure 5). The relative intensity ratio indeed depends on the respective thickness ratios of these sublayers and from the sharpness of the various interfaces (i.e., the quality of the microsegregation). A rough estimation of the volume of the rodlike yttrium complex at 120 °C, obtained by addition of partial volume $\{V_{mol} = V(\mathbf{L6}) + 2V([Y(hfac)_3]) \approx 6200 + 1800 = 8000$ Å$^2\}$,[25] gives a molecular area of $A_{mol} = V_{mol}/d = 76$ Å^2 (e.g., a value that corresponds to an area per cyanobiphenyl of 38 Å^2), which is significantly larger than the cross-section of an aliphatic chain (22.5 Å^2). Altogether, the shorter lamellar periodicity and the larger molecular area can be traced back to a considerable tilt angle of the peripheral and internal mesogens and consequently to the undulation of the layers at the mesogen–mesogen interface. A possible model for the supramolecular organisation of the complexes into a lamellar structure would consist of their lateral arrangement primarily induced by the segregation of the chelating part to form the central sublayer. On either side of that sublayer are first disposed a mixed stratum including aliphatic spacers and branching mesogen, followed by terminal cyanobiphenyls. The large surface area is compensated by large undulations of the layer, which is equivalent at the molecular level to an average important

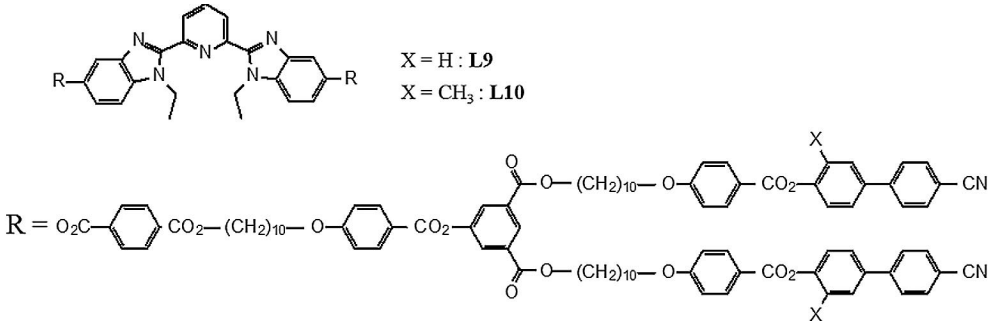

tilt angle of the mesogens to reach the 38 Å^2 target area for a terminal cyanobiphenyl.

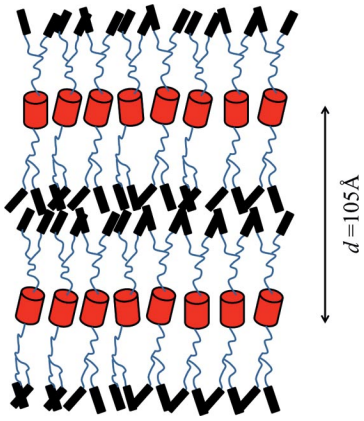

Figure 5. Proposed SmA-like organisation for $[Y_2(\mathbf{L6})(hfac)_6]$. The red cylinders are the metallic cores of the complexes, the blue lines are the dendritic spacer and the black rectangles are the terminal cyanobiphenyl mesogens.

Further insight into the organisation of the cyanobiphenyl units at the interface can be gained by monitoring the C≡N stretching vibration (ν_{CN}) during the crystal–liquid to isotropic liquid phase transitions.[26] Interestingly, ν_{CN} is particularly sensitive to changes in intermolecular CN···CN interactions that occur at the phase transitions[27] but the temperature dependence (20–200 °C) of both frequency (ν_{CN} [cm^{-1}]) and integrated intensities (I_{CN} in the 2200 to 2250 cm^{-1} range)[28] of the CN stretching band in $[Y_2(\mathbf{L6})(hfac)_6]$ during the isotropisation process shows no abrupt variation (Figures S27 and S28 in the Supporting Information) except during the first heating, in which cocrystallised water molecules are expulsed (Figures S29–32 in the Supporting Information). We conclude that, as expected from the large molecular area estimated at the interface, the terminal cyano groups are not significantly involved in the stabilisation of the SmA phase in $[Y_2(\mathbf{L6})(hfac)_6]$. On the contrary, a significant and abrupt change of ν_{CN} was measured for ligand **L6** at the N→I transition (Figures S33 and S34 in the Supporting Information). The weaker constraints in the nematic phase of **L6** make the CN groups of the ligand free enough to interact with neighbouring groups, thus contributing to the stabilisation of the mesophase.

Conclusion

The drastic decrease in stability previously reported for lipophilic d-block liquid-crystalline helicates $[Cu_2(\mathbf{L4}n)_2]^{2+}$ (n = a, b, c)[17] is strictly mirrored by f-block helicates. The special anchoring of the dendrimeric residues perpendicular to the helical axis excludes the operation of significant repulsive interstrand steric effects, and the instability of the lipophilic complexes $[Ln_2(\mathbf{L5})_3](CF_3SO_3)_6$ (Ln = La, Y, Lu) and $[Y_2(\mathbf{L6})_3](CF_3SO_3)_6$ in CD_2Cl_2/CD_3CN can be unambiguously assigned to the efficient solvation of the lipophilic receptors **L**k (k = 5, 6) in organic solvents. With this in mind, the limited stability of multistranded complexes can be exploited for the alternative selective preparation of the dinuclear single-stranded complex $[Y_2(\mathbf{L6})(hfac)_6]$ in the absence of higher-order helicates. The rigid metallic core modelled by $[Y_2(\mathbf{L1})(hfac)_6]$ (helicity index = 0.55) has a cylindrical shape with a 50–80 Å^2 cross-section and 25 Å length (Figure S36 in the Supporting Information). Its dendritic lipophilic version found in $[Y_2(\mathbf{L6})(hfac)_6]$ self-organises just above room temperature to give a SmA-type liquid-crystalline phase. To the best of our knowledge, $[Y_2(\mathbf{L6})(hfac)_6]$ is the first reported rodlike dinuclear lanthanidomesogen.

Experimental Section

General: Chemicals were purchased from Acros, Alfa Aesar and Aldrich, and used without further purification unless otherwise stated. The trifluoromethanesulfonate $[Ln(CF_3SO_3)_3]\cdot xH_2O$[29] and hexafluoroacetylacetonate $[Ln(hfac)_3(diglyme)]$[30] salts were prepared from the corresponding oxide (Aldrich, 99.99%). The Ln contents of solid salts were determined by complexometric titrations with Titriplex III (Merck) in the presence of urotropine and xylene orange.[31] Acetonitrile and dichloromethane were distilled from calcium hydride. Methanol was distilled from $Mg(OCH_3)_2$. Silica gel plates Merck 60 F254 were used for thin-layer chromatography (TLC) and Fluka silica gel 60 (0.04–0.063 mm) was used for preparative column chromatography.

Preparation of L5: Anhydrous K_2CO_3 (0.12 g, 0.87 mmol) and a catalytic amount of KI (50 mg) were added to a solution of **11** (0.10 g, 0.15 mmol) and **15** (0.24 g, 0.35 mmol) in DMF (20 mL). The reaction mixture was stirred at 60 °C for 24 h under a nitrogen atmosphere. The reaction mixture was evaporated to dryness and the resulting oily mixture was partitioned between CH_2Cl_2/half-saturated NaCl (100 mL:100 mL). The organic phase was separated, dried with anhydrous $MgSO_4$, filtered and the solvents were evaporated to dryness. The product was purified by column chromatography [silica gel (50 g), CH_2Cl_2/MeOH 100:0, 99.5:0.5, 99:1 and 98.5:1.5] and dried for 24 h under vacuum at 80 °C to yield **L5** (0.170 g, 8.68×10^{-5} mol, 60%) as a white oil that solidified after several days. ^{1}H NMR (400 MHz, $CDCl_3$): δ = 0.90 (t, ^3J = 6.8 Hz, 12 H), 1.10 (t, ^3J = 7.1 Hz, 6 H), 1.23–1.52 (m, 112 H), 1.72–1.89 (m, 16 H), 3.38 (q, ^3J = 7.1 Hz, 4 H), 3.61 (q, ^3J = 7.1 Hz, 4 H), 3.92 (t, ^3J = 6.6 Hz, 12 H), 4.12–4.12 (br., 4 H), 4.30 (s, 2 H), 4.77 (q, ^3J = 6.8 Hz, 4 H), 6.08 (s, 6 H), 7.07 (d, ^4J = 2.0 Hz, 2 H), 7.24 (d, ^3J = 8.0 Hz, 2 H), 7.37 (d, ^3J = 8.0 Hz, 2 H), 7.72 (s, 2 H), 7.89 (s, 2 H) ppm. ESI-MS (CH_2Cl_2/MeOH, 9:1): m/z = 960.5 $[M + 2H]^{2+}$, 1919.9 $[M + H]^+$. $C_{121}H_{192}N_8O_{10}$ (1918.90): calcd. C 75.61, H 9.95, N 8.39; found C 75.74, H 10.09, N 8.34.

Preparation of L6: 1-Ethyl-3-(3-dimethylaminopropyl)carbodiimide hydrochloride (EDCI·HCl; 0.033 g, 1.74×10^{-4} mol), and 4-dimethylaminopyridine (DMAP; catalytic) were added to a solution of **16** (0.145 g, 9.58×10^{-5} mol) in CH_2Cl_2 (40 mL) under an inert atmosphere. The solution was stirred at room temp. for 5 min and compound **10** (0.030 g, 4.36×10^{-5} mol) was added. The reaction mixture was heated at reflux for 12 h [the progression of the reaction was monitored by TLC (CH_2Cl_2/MeOH, 98:2)]. The reaction mixture was then diluted to 100 mL with CH_2Cl_2, washed with a half-saturated aqueous solution of NaCl (3×50 mL), dried with anhydrous Na_2SO_4, filtered and the solvents evaporated to dryness. The crude product was purified by column chromatography [silica gel (75 g), CH_2Cl_2/MeOH 100:0, 99.5:0.5, 99:1]. Finally, the product

was dissolved in CH_2Cl_2 (2 mL) and this solution was then poured into MeOH (50 mL). The precipitate was filtered using a membrane (45 μm porosity), washed with MeOH and dried under vacuum at 80 °C for 12 h to yield **L6** (0.099 g, 2.70×10^{-5} mol, 62%) as a white solid. ^{1}H NMR (400 MHz, $CDCl_3$): δ = 1.15 (t, ^3J = 7.0 Hz, 6 H), 1.31 (t, ^3J = 7.1 Hz, 6 H), 1.33–1.54 (m, 78 H), 1.75–1.88 (m, 24 H), 3.44 (q, ^3J = 7.0 Hz, 4 H), 3.64 (q, ^3J = 7.1 Hz, 4 H), 4.06 (t, ^3J = 6.5 Hz, 8 H), 4.07 (t, ^3J = 6.5 Hz, 4 H), 4.30 (s, 2 H), 4.37 (t, ^3J = 6.8 Hz, 8 H), 4.39 (t, ^3J = 6.8 Hz, 4 H), 4.81 (q, ^3J = 7.2 Hz, 4 H), 7.00 (d, ^3J = 9.1 Hz, 8 H),7.01 (t, ^3J = 9.1 Hz, 4 H), 7.26 (dd, ^3J = 8.5 Hz, ^4J = 1.5 Hz, 2 H), 7.34 (d, ^3J = 8.9 Hz, 8 H), 7.39 (d, ^3J = 8.5 Hz, 2 H), 7.58 (d, ^4J = 2.2 Hz, 2 H), 7.65 (d, ^3J = 9.1 Hz, 8 H), 7.69–7.72 (m, 10 H), 7.74–7.77 (m, 8 H), 8.08 (d, ^4J = 1.5 Hz, 4 H), 8.17 (d, ^3J = 9.1 Hz, 4 H), 8.18 (d, ^3J = 9.1 Hz, 8 H), 8.21 (d, ^3J = 8.8 Hz, 4 H), 8.28 (d, ^3J = 8.8 Hz, 4 H), 8.38 (d, ^4J = 2.2 Hz, 2 H), 8.61 (t, ^4J = 1.5 Hz, 2 H) ppm. ESI-MS (CH_2Cl_2/MeOH, 9:1): *m*/*z* = 3681.4 [M + H]$^+$. $C_{225}H_{232}N_{12}O_{36}$·18.01, H_2O: calcd. C 67.48, H 6.75, N 4.20; found C 67.48, H 6.75, N 4.20. The hydration was confirmed by TGA (Figure S20a in the Supporting Information).

Preparation of Complex [Y_2(L6)(hfac)$_6$]: Ligand **L6** (30 mg, 8.15×10^{-6} mol; 1 equiv.) was treated with anhydrous [Y(hfac)$_3$(diglyme)] (2.0 equiv.) in $CHCl_3$ (2 mL) at room temperature. After 1 h stirring, hexane (4 mL) was added and a white precipitate formed. The suspension was centrifuged (5000 rpm, 10 min) and the solvent was removed. This procedure was repeated twice. The white solid was dried under vacuum at 80 °C for 12 h, thereby quantitatively yielding the expected [Y_2(**L6**)(hfac)$_6$] complex (Table S1 in the Supporting Information).

Spectroscopic and Analytical Measurements: ^{1}H and ^{13}C NMR spectra were recorded at 298 K with a Bruker Avance 400 MHz spectrometer. Chemical shifts are given in ppm with respect to TMS. Pneumatically assisted electrospray (ESI-MS) mass spectra were recorded from 10^{-4} M solutions with an Applied Biosystems API 150EX LC/MS System equipped with a Turbo Ionspray source. Elemental analyses were performed by K. L. Buchwalder of the University of Geneva. The variable-temperature FTIR spectra were recorded with an IRTF Nicolet iS10 spectrometer in diffuse reflectance mode by using a high-temperature diffuse reflectance environmental chamber. The samples were diluted into a KBr matrix and the resulting mixtures that contained about 10% of compound were ground before being heated at 200 °C for a few minutes. After cooling to room temperature, the FTIR spectra were recorded in the 20–200 °C and 200–20 °C temperature ranges by using a heating or cooling rate of 2 °C min^{-1}. The spectra were recorded with a resolution of 0.4 cm^{-1}. TGA was performed with a Seiko TG/DTA 320 thermogravimetric balance (under N_2). DSC traces were obtained with a Mettler Toledo DSC1 Star Systems differential scanning calorimeter from 3 to 5 mg samples (5 °C min^{-1} under N_2). Characterisation of the mesophases was performed with a Leitz OrthoplanPol polarising microscope with a Leitz LL 20×/0.40 polarising objective and equipped with a Linkam THMS 600 variable-temperature stage. The SAXRD patterns were obtained with three different experimental setups, and in all cases the crude powder was filled in Lindemann capillaries that were 1 mm in diameter: (1) A STOE STADI P transmission powder diffractometer system using a focused monochromatic Cu-$K_{\alpha 1}$ beam obtained from a curved germanium monochromator (Johann-type) and collected on a curved image-plate position-sensitive detector. A calibration with silicon and copper laurate standards for high- and low-angle domains, respectively, was performed preliminarily. Sample capillaries were placed in the high-temperature attachment for measurements in the range of desired temperatures (from 20 to 160 °C), for which the sample temperature was controlled within 0.05 °C. (2) An image plate. The cell parameters were calculated from the position of the reflection at the smallest Bragg angle, which was in all cases the most intense. Periodicities up to 150 Å could be measured, and the sample temperature was controlled within a temperature range of 0.3 °C. The exposure times were varied from 2 to 6 h, depending on the specific reflections sought (weaker reflections clearly taking longer exposure times). (3) An SAXS system from Molecular Metrology equipped with a Cu-$K_{\alpha 1}$ Bede microsource conditioned with confocal MaxFluxTM optics and a two-dimensional multiwire gas detector. A modified temperature stage from Linkham was used to control the temperatures. The computational analysis was performed with MatLab-based open-source software from Molecular Metrology.

X-ray Crystallography: Summary of crystal data, intensity measurements and structure refinements for **10** and [Lu_2(**L1**)(hfac)$_6$] are collected in Tables S2 and S4 (in the Supporting Information). Crystals were mounted on a quartz fibre with protection oil. Cell dimensions and intensities were measured at 180 K with a Stoe IPDS diffractometer with graphite-monochromated Mo-K_α radiation (λ = 0.71073 Å) for **10** and at 180 K with a Supernova (Agilent) diffractometer using mirror-monochromated Cu-K_α radiation (λ = 1.5418 Å) for [Lu_2(**L1**)(hfac)$_6$]. Data were corrected for Lorentz and polarisation effects and for absorption. The structure was solved by direct methods (SIR97)[32] or SHELXS;[33] all other calculation were performed with SHELXL97[33] and ORTEP[34] software.

CCDC-905224 (for **10**) and -905225 (for [Lu_2(**L1**)(hfac)$_6$]) contain the supplementary crystallographic data for this paper. These data can be obtained free of charge from The Cambridge Crystallographic Data Centre via www.ccdc.cam.ac.uk/data_request/cif.

Comments on the Crystal Structure of 10: Precursory ligand **10** crystallised in a monoclinic system (space group *C*2/*c*) with one independent molecule in the asymmetric unit (Z = 8). There was one additional nitromethane solvent molecule. Atoms C17, C16 and C26 were disordered and refined over two sites with occupancy factors of 0.52/0.48, 0.61/0.39 and 0.47/0.53, respectively, and with constrained isotropic displacement parameters. The positions of hydrogen atoms were calculated and refined with restraints on bond lengths and bond angles. Intermolecular π stacking were observed (1) between planar aromatic benzimidazole rings related by an inversion centre (d = 3.615Å, shift distance = 0.863Å) and (2) between a phenyl ring and a benzimidazole ring (d = 3.67Å, angle between planes = 4.69°). There were three intermolecular π-stacking interactions per molecule (Figure S1b in the Supporting Information).

Comments on the Crystal Structure of [Lu_2(L1)(hfac)$_6$]: Crystallisation of complex [Lu_2(**L1**)(hfac)$_6$] in the triclinic $P\bar{1}$ space group gave small colourless prismatic crystals. The measured small crystal is a two nonmerohedral twin (the ratio of the twin components is 0.47:0.53). No solvate molecules were found in the structure. Some CF_3 groups of the coordinated hfac counterions were disordered (rotation about the threefold axes) and therefore displayed large anisotropic ellipsoids. The three most disordered CF_3 groups were refined by splitting each F atom on two sites with restraints on bond lengths and on bond angles. Their displacement parameters were refined isotropically and constrained to be equal. Occupancy factors were refined and converge to values of around 0.5. Hydrogen atoms were calculated and refined with restraints on bond lengths and bond angles.

Supporting Information (see footnote on the first page of this article): This includes Schemes S1 and S2, Figures S1–S36 and Tables S1–S11.

Acknowledgments

Financial support from the Swiss National Science Foundation is gratefully acknowledged. S. F. acknowledges the Centre National de la Recherche Scientifique (CNRS), the Ministère de l'Enseignement Supérieur et de la Recherche (MESR) and C'Nano Ile de France through the project ECOPOMs 2009 for financial support.

[1] a) C. Piguet, J.-C. G. Bünzli, G. Bernardinelli, G. Hopfgartner, A. F. Williams, *J. Am. Chem. Soc.* **1993**, *115*, 8197–8206; b) N. Martin, J.-C. G. Bünzli, V. McKee, C. Piguet, G. Hopfgartner, *Inorg. Chem.* **1998**, *37*, 577–589; c) S. Floquet, N. Ouali, B. Bocquet, G. Bernardinelli, D. Imbert, J.-C. G. Bünzli, G. Hopfgartner, C. Piguet, *Chem. Eur. J.* **2003**, *9*, 1860–1875; d) K. Zeckert, J. Hamacek, J.-M. Senegas, N. Dalla-Favera, S. Floquet, G. Bernardinelli, C. Piguet, *Angew. Chem.* **2005**, *117*, 8168; *Angew. Chem. Int. Ed.* **2005**, *44*, 7954–7958; e) C. Piguet, J.-C. G. Bünzli, in *Handbook on the Physics and Chemistry of Rare Earths*, Vol. 40 (Eds.: K. A. Gschneidner Jr, J.-C. G. Bünzli, V. K. Pecharsky), Elsevier Science, Amsterdam, **2009**, pp. 301–553; f) C. Lincheneau, F. Stomeo, S. Comby, T. Gunnlaugsson, *Aust. J. Chem.* **2011**, *64*, 1315–1326; g) S. Zebret, C. Besnard, G. Bernardinelli, J. Hamacek, *Eur. J. Inorg. Chem.* **2012**, 2409–2417; h) H.-F. Li, P.-F. Yan, P. Chen, Y. Wang, H. Xu, G.-M. Li, *Dalton Trans.* **2012**, *41*, 900–907.

[2] a) M. P. Oude Wolbers, F. C. J. M. van Veggel, F. G. A. Peters, E. S. E. van Beelen, J. W. Hofstraat, F. A. J. Geurts, D. N. Reinhoudt, *Chem. Eur. J.* **1998**, *4*, 772–780; b) J. Hamacek, G. Bernardinelli, Y. Filinchuk, *Eur. J. Inorg. Chem.* **2008**, 3419–3422; c) B. El Aroussi, L. Guénée, P. Pal, J. Hamacek, *Inorg. Chem.* **2011**, *50*, 8588–8597; d) J. Xu, T. M. Corneillie, E. G. Moore, G.-L. Law, N. G. Butlin, K. N. Raymond, *J. Am. Chem. Soc.* **2011**, *133*, 19900–19910; e) J. Hamacek, D. Poggiali, S. Zebret, B. El Aroussi, M. W. Schneider, M. Mastarlez, *Chem. Commun.* **2012**, *48*, 1281–1283.

[3] a) J. Xu, K. N. Raymond, *Angew. Chem.* **2000**, *112*, 2857; *Angew. Chem. Int. Ed.* **2000**, *39*, 2745–2747; b) Z. Zheng, *Chem. Commun.* **2001**, 2251–2259; c) D. Chapon, P. Delangle, C. Lebrun, *J. Chem. Soc., Dalton Trans.* **2002**, 68–74; d) S. Delagrange, C. Gateau, D. Chapon, C. Lebrun, P. Delangle, P. Vottéro, *Eur. J. Inorg. Chem.* **2002**, 2991–2998; e) D. Chapon, J.-P. Morel, P. Delangle, C. Gateau, J. Pécaut, *Dalton Trans.* **2003**, 2745–2749; f) N. Ouali, J.-P. Rivera, D. Chapon, P. Delangle, C. Piguet, *Inorg. Chem.* **2004**, *43*, 1517–1529; g) T. Kajiwara, H. Wu, T. Ito, N. Iki, S. Miyano, *Angew. Chem.* **2004**, *116*, 1868; *Angew. Chem. Int. Ed.* **2004**, *43*, 1832–1835; h) X. Yng, R. A. Jones, *J. Am. Chem. Soc.* **2005**, *127*, 7686–7687; i) O. Mamula, M. Lama, H. Stoeckli-Evans, S. Shova, *Angew. Chem.* **2006**, *118*, 5062; *Angew. Chem. Int. Ed.* **2006**, *45*, 4940–4944; j) X.-Y. Chen, Y. Bretonnière, J. Pécaut, D. Imbert, J.-C. G. Bünzli, M. Mazzanti, *Inorg. Chem.* **2007**, *46*, 625–637.

[4] M. A. Anwar, L. K. Thompson, L. N. Dave, F. Habib, M. Murugesu, *Chem. Commun.* **2012**, *48*, 4576–4578.

[5] a) D.-J. Qian, K.-Z. Yang, H. Nakahara, K. Fukuda, *Langmuir* **1997**, *13*, 5925–5932; b) K. Binnemans, C. Görller-Walrand, *Chem. Rev.* **2002**, *102*, 2303–2346; c) C. Piguet, J.-C. G. Bünzli, B. Donnio, D. Guillon, *Chem. Commun.* **2006**, 3755–3768; d) M. Burnworth, D. Knapton, S. J. Rowan, C. Weder, *J. Inorg. Organomet. Polym. Mater.* **2007**, *17*, 91–103; e) B. Donnio, S. Buathong, I. Bury, D. Guillon, *Chem. Soc. Rev.* **2007**, *36*, 1495–1513; f) K. Binnemans, *J. Mater. Chem.* **2009**, *19*, 448–453; g) K. Binnemans, *Chem. Rev.* **2009**, *109*, 4283–4374; h) B. M. McKenzie, R. J. Wojtecki, K. A. Burke, C. Zhang, A. Jakli, P. T. Mather, S. J. Rowan, *Chem. Mater.* **2011**, *23*, 3525–3533.

[6] R. L. Carrol, C. B. Gorman, *Angew. Chem. Int. Ed.* **2002**, *41*, 4379–4400.

[7] a) A. M. Giroud-Godquin, P. M. Maitlis, *Angew. Chem.* **1991**, *103*, 370; *Angew. Chem. Int. Ed. Engl.* **1991**, *30*, 375–402; b) D. W. Bruce, *J. Chem. Soc., Dalton Trans.* **1993**, 2983–2989; c) S. A. Hudson, P. M. Maitlis, *Chem. Rev.* **1993**, *93*, 861–885; d) J. L. Serrano, *Metallomesogens, Synthesis Properties and Applications*, VCH, Weinheim, Germany, **1996**; e) P. Espinet, M. A. Esteruelas, L. A. Oro, J.-L. Serrano, E. Sola, *Coord. Chem. Rev.* **1992**, *117*, 215–274; f) B. Donnio, D. W. Bruce, *Struct. Bonding (Berlin)* **1999**, *95*, 194–247; g) B. Donnio, D. Guillon, R. Deschenaux, D. W. Bruce, in *Comprehensive Coordination Chemistry* (Eds.: J. A. McCleverty, T. J. Meyer), Elsevier, Oxford, U.K. **2003**, vol. 7, chapter 79.

[8] K. Binnemans, in: *Handbook on the Physics and Chemistry of Rare Earths*, vol. 43 (Eds.: J.-C. G. Bünzli, V. K. Pecharsky), Elsevier BV, Burlington, **2013**, chapter 254, p. 1–158.

[9] *Handbook of Liquid Crystals* (Eds.: D. Demus, J. W. Goodby, G. W. Gray, H.-W. Spiess, V. Vill), Wiley-VCH, Weinheim, Germany, **1998**.

[10] A. Skoulios, D. Guillon, *Mol. Cryst. Liq. Cryst.* **1988**, *165*, 317–332.

[11] K. J. Toyne, *Thermotropic Liquid Crystals* (Ed.: G. W. Gray), Critical Reports on Applied Chemistry, Wiley, Chichester, UK, **1987**, vol. 22, pp. 28–63.

[12] R. W. Date, E. Fernandez Iglesias, K. E. Rowe, J. M. Elliott, D. W. Bruce, *Dalton Trans.* **2003**, 1914–1931.

[13] a) F. Neve, M. Ghedini, G. De Munno, A. M. Levelut, *Chem. Mater.* **1995**, *7*, 688–693; b) L. Douce, A. El-ghayouri, A. Skoulios, R. Ziessel, *Chem. Commun.* **1999**, 2033–2034; c) R. Gimenez, A. B. Manrique, S. Uriel, J. Barbera, J. L. Serrano, *Chem. Commun.* **2004**, 2064–2065; d) E. Cavero, S. Uriel, P. Romero, J. L. Serrano, R. Gimenez, *J. Am. Chem. Soc.* **2007**, *129*, 11608–11618; e) R. Ziessel, G. Pickaert, F. Camerel, B. Donnio, D. Guillon, M. Cesario, T. Prange, *J. Am. Chem. Soc.* **2004**, *126*, 12403–12413; f) E. D. Baranoff, J. Voignier, T. Yasuda, V. Heitz, J.-P. Sauvage, T. Kato, *Angew. Chem.* **2007**, *119*, 4764; *Angew. Chem. Int. Ed.* **2007**, *46*, 4680–4683; g) D. Pucci, I. Aiello, A. Bellusci, A. Crispini, M. Ghedini, M. La Deda, *Eur. J. Inorg. Chem.* **2009**, 4274–4281.

[14] a) G. Lattermann, S. Schmidt, R. Kleppinger, J. H. Wendorf, *Adv. Mater.* **1992**, *4*, 30–33; b) S. Schmidt, G. Lattermann, R. Kleppinger, J. H. Wendorff, *Liq. Cryst.* **1994**, *16*, 693–702; c) H. Zheng, T. M. Swager, *J. Am. Chem. Soc.* **1994**, *116*, 761–762; d) X.-H. Liu, M. N. Abser, D. W. Bruce, *J. Organomet. Chem.* **1998**, *551*, 271–280; e) G. H. Walf, R. Benda, F. J. Litterst, U. Stebani, S. Schmidt, G. Lattermann, *Chem. Eur. J.* **1998**, *4*, 93–99; f) K. E. Rowe, D. W. Bruce, *J. Chem. Soc., Dalton Trans.* **1996**, 3913–3915; g) S. Morrone, D. Guillon, D. W. Bruce, *Inorg. Chem.* **1996**, *35*, 7041–7048; h) F. Camerel, R. Ziessel, B. Donnio, D. Guillon, *New J. Chem.* **2006**, *30*, 135–139; i) A. M. Prokhorov, A. Santoro, J. A. G. Williams, D. W. Bruce, *Angew. Chem.* **2012**, *124*, 99; *Angew. Chem. Int. Ed.* **2012**, *51*, 95–98; j) Y. Galyametdinov, V. Ksenofontov, A. Prosvirin, I. Ovchinnikov, G. Ivanova, P. Gütlich, W. Haase, *Angew. Chem.* **2001**, *113*, 4399; *Angew. Chem. Int. Ed.* **2001**, *40*, 4269–4271; k) F. Camerel, J. Barberá, J. Otsuki, T. Tokimoto, Y. Shimazaki, L.-Y. Chen, S.-H. Liu, M.-S. Lin, C.-C. Wu, R. Ziessel, *Adv. Mater.* **2008**, *20*, 3462–3467; l) T. Cardinaels, J. Ramaekers, K. Driesen, P. Nockemann, K. Van Hecke, L. Van Meervelt, B. Goderis, K. Binnemans, *Inorg. Chem.* **2009**, *48*, 2490–2499; m) S. Frein, M. Auzias, A. Sondenecker, L. Vieille-Petit, B. Guintchin, N. Maringa, G. Süss-Fink, J. Barbera, R. Deschenaux, *Chem. Mater.* **2008**, *20*, 1340–1343; n) E. Terazzi, C. Bourgogne, R. Welter, J.-L. Gallani, D. Guillon, G. Rogez, B. Donnio, *Angew. Chem.* **2008**, *120*, 500; *Angew. Chem. Int. Ed.* **2008**, *47*, 490–495.

[15] a) E. Terazzi, S. Torelli, G. Bernardinelli, J.-P. Rivera, J.-M. Bénech, C. Bourgogne, B. Donnio, D. Guillon, D. Imbert, J.-C. G. Bünzli, A. Pinto, D. Jeannerat, C. Piguet, *J. Am. Chem.*

Soc. **2005**, *127*, 888–903; b) K. Binnemans, K. Lodewyckx, B. Donnio, D. Guillon, *Eur. J. Inorg. Chem.* **2005**, 1506–1513; c) H. Nozary, S. Torelli, L. Guénée, E. Terazzi, G. Bernardinelli, B. Donnio, D. Guillon, C. Piguet, *Inorg. Chem.* **2006**, *45*, 2989–3003; d) K. Binnemans, K. Lodewyckx, T. Cardinaels, T. N. Parac-Vogt, C. Bourgogne, D. Guillon, B. Donnio, *Eur. J. Inorg. Chem.* **2006**, 150–157; e) Y. Yang, K. Driesen, P. Nockemann, K. Van Hecke, L. Van Meervelt, K. Binnemans, *Chem. Mater.* **2006**, *18*, 3698–3704; f) E. Terazzi, L. Guénée, P.-Y. Morgantini, G. Bernardinelli, B. Donnio, D. Guillon, C. Piguet, *Chem. Eur. J.* **2007**, *13*, 1674–1691; g) A. Escande, L. Guénée, H. Nozary, G. Bernardinelli, F. Gumy, A. Aebischer, J.-C. G. Bünzli, B. Donnio, D. Guillon, C. Piguet, *Chem. Eur. J.* **2007**, *13*, 8696–8713; h) T. Cardinaels, K. Driesen, T. N. Parac-Vogt, B. Heinrich, C. Bourgogne, D. Guillon, B. Donnio, K. Binnemans, *Chem. Mater.* **2005**, *17*, 6589–6598; i) E. Terazzi, B. Bocquet, S. Campidelli, B. Donnio, D. Guillon, R. Deschenaux, C. Piguet, *Chem. Commun.* **2006**, 2922–2924; j) T. B. Jensen, E. Terazzi, B. Donnio, D. Guillon, C. Piguet, *Chem. Commun.* **2008**, 181–183; k) A. A. Knyazev, Y. G. Galyametdinov, B. Goderis, K. Driesen, K. Goossens, C. Görller-Walrand, K. Binnemans, T. Cardinaels, *Eur. J. Inorg. Chem.* **2008**, 756–761; l) T. B. Jensen, E. Terazzi, K.-L. Buchwalder, L. Guénée, H. Nozary, K. Schenk, B. Heinrich, B. Donnio, D. Guillon, C. Piguet, *Inorg. Chem.* **2010**, *49*, 8601–8619.

[16] B. Dardel, D. Guillon, B. Heinrich, R. Deschenaux, *J. Mater. Chem.* **2001**, *11*, 2814–2831.

[17] a) A. El-ghayoury, L. Douce, A. Skoulios, R. Ziessel, *Angew. Chem.* **1998**, *110*, 2327; *Angew. Chem. Int. Ed.* **1998**, *37*, 2205–2208; b) R. Ziessel, L. Douce, A. El-ghayoury, A. Harriman, A. Skoulios, *Angew. Chem.* **2000**, *112*, 1549; *Angew. Chem. Int. Ed.* **2000**, *39*, 1489–1493.

[18] K. Zeckert, J. Hamacek, J.-P. Rivera, S. Floquet, A. Pinto, M. Borkovec, C. Piguet, *J. Am. Chem. Soc.* **2004**, *126*, 11589–11601.

[19] a) C. Piguet, G. Bernardinalli, G. Hopfgartner, *Chem. Rev.* **1997**, *97*, 2005–2062; b) M. Albrecht, *Chem. Rev.* **2001**, *101*, 3457–3497.

[20] A. Zaïm, H. Nozary, L. Guénée, C. Besnard, J.-F. Lemonnier, S. Petoud, C. Piguet, *Chem. Eur. J.* **2012**, *18*, 7155–7168.

[21] a) A. Escande, L. Guénée, K.-L. Buchwalder, C. Piguet, *Inorg. Chem.* **2009**, *48*, 1132–1147; b) I. D. Brown, D. Altermatt, *Acta Crystallogr., Sect. B* **1985**, *41*, 244–247; c) N. E. Breese, M. O'Keeffe, *Acta Crystallogr., Sect. B* **1991**, *47*, 192–197; d) I. D. Brown, *Acta Crystallogr., Sect. B* **1992**, *48*, 553–572; e) I. D. Brown, *The Chemical Bond in Inorganic Chemistry*, Oxford University Press, UK, **2002**; f) I. D. Brown, *Chem. Rev.* **2009**, *109*, 6858–6919; g) A. Trzesowska, R. Kruszynski, T. J. Bartczak, *Acta Crystallogr., Sect. B* **2004**, *60*, 174–178; h) A. Trzesowska, R. Kruszynski, T. J. Bartczak, *Acta Crystallogr., Sect. B* **2005**, *61*, 429–434; i) F. J. Zocchi, *Mol. Struct. A* **2007**, *805*, 73–78.

[22] $H = 6\sqrt{3}\pi\frac{LA}{D^3}$ with L = 4.06 Å is the end-to-end distance of the helix taken as the C15···C27 contact distance. A = 0.80 Å^2 is the area of the quadrangle produced by the projection of the five atoms of the diphenylmethane spacer onto a plane perpendicular to the main helical axis defined as the line passing through the two terminal atoms of the chain. Finally, D = 5.78 Å is the length of the crooked line: J. H. Brewster, *Top. Curr. Chem.* **1974**, *46*, 29–71.

[23] N. Dalla Favera, L. Guénée, G. Bernardinelli, C. Piguet, *Dalton Trans.* **2009**, 7625–7638.

[24] *HypNMR-2008 software*: a) C. Frassineti, S. Ghelli, P. Gans, A. Sabatini, M. S. Moruzzi, A. Vacca, *Anal. Biochem.* **1995**, *231*, 374–382; b) C. Frassineti, L. Alderighi, P. Gans, A. Sabatini, A. Vacca, S. Ghelli, *Anal. Bioanal. Chem.* **2003**, *376*, 1041–1052.

[25] The volume of [Y(hfac)$_3$] was estimated from that of [Y(acac)$_3$], see: J. A. Cunningham, D. E. Sands, W. F. Wagner, *Inorg. Chem.* **1967**, *6*, 499–503.

[26] K. Hori, M. Kuribayashi, M. Iimuro, *Phys. Chem. Chem. Phys.* **2000**, *2*, 2863–2868, and references cited therein.

[27] P. A. Wood, S. J. Borwick, D. J. Watkin, W. D. S. Motherwell, F. H. Allen, *Acta Crystallogr., Sect. B* **2008**, *64*, 393–396.

[28] D. Steele, in: *Handbook of Vibrational Spectroscopy*, vol. 1 (Eds.: J. M. Chalmers, P. R. Griffiths), Wiley, Chichester, UK, **2002**, chapter 3.

[29] J. F. Desreux, in: *Lanthanide Probes in Life, Chemical and Earth Sciences* (Eds.: J.-C. G. Bünzli, G. R. Choppin), Elsevier, Amsterdam, **1989**, chapter 2, p. 43.

[30] a) W. J. Evans, D. G. Giarikos, M. A. Johnston, M. A. Greci, J. W. Ziller, *J. Chem. Soc., Dalton Trans.* **2002**, 520–526; b) G. Malandrino, R. Lo Nigro, I. L. Fragala, C. Benelli, *Eur. J. Inorg. Chem.* **2004**, 500–509.

[31] G. Schwarzenbach, *Complexometric Titrations*, Chapman & Hall, London, **1957**, p. 8.

[32] A. Altomare, M. C. Burla, M. Camalli, G. Cascarano, C. Giacovazzo, A. Guagliardi, G. Moliterni, G. Polidori, R. Spagna, *J. Appl. Crystallogr.* **1999**, *32*, 115–119.

[33] SHELXL97, G. M. Sheldrick, *Acta Crystallogr. A* **2008**, *A64*, 112–122.

[34] *ORTEP-III for Windows*, J. L. Farrugia, *J. Appl. Crystallogr.* **1997**, *30*, 565.

Received: February 4, 2013
Published Online: April 22, 2013

